

Anticorrelated Hard/Soft X-ray Emission from the X-Ray Burster 4U 0614+091

E. Ford¹, P. Kaaret¹, M. Tavani¹, B.A. Harmon², S.N. Zhang³, D. Barret⁴, J. Grindlay⁴, P. Bloser⁴, R. A. Remillard⁵

ABSTRACT

We have detected transient X-ray activity from the X-ray burster 4U 0614+091 simultaneously with BATSE/CGRO (20–100 keV) and ASM/RXTE (1–12 keV). The peak fluxes reach approximately 40 mCrab in both instruments over a period of about 20 days. The variable emission shows a clear anticorrelation of the hard X-ray flux with the soft X-ray count rate. The observed anticorrelation is another clear counterexample to the notion that only black hole binaries exhibit such correlations. The individual spectra during this period can be fit by power laws with photon indices 2.2 ± 0.3 (ASM) and 2.7 ± 0.4 (BATSE), while the combined spectra can be described by a single power law with index 2.09 ± 0.08 . BATSE and the ASM/RXTE are a good combination for monitoring X-ray sources over a wide energy band.

Subject headings: accretion, accretion disks — stars: individual (4U 0614+091)
— stars: neutron — X-rays: stars

¹Columbia University, Department of Physics and Columbia Astrophysics Lab, 538 W. 120th Street, New York, NY 10027

²NASA/Marshall Space Flight Center, ES 84, Huntsville, AL 35812

³University Space Research Association/ MSFC, ES 84, Huntsville, AL 35812

⁴Harvard Smithsonian Center for Astrophysics, 60 Garden Street, Cambridge, MA 02138

⁵MIT, Center for Space Science, Room 37-595, Cambridge, MA 02139

1. Introduction

Many X-ray emission properties once thought to uniquely characterize black hole candidates have now been observed in systems containing weakly magnetized neutron stars (e.g. Barret and Vedrenne 1994; van der Klis 1994; Inoue 1990). A classic observational feature of black hole candidates (BHCs) has been the presence of hard power law tails in the energy spectra extending above 100 keV. Typically the hard X-ray emission is anti-correlated with soft X-ray luminosity (Tanaka 1989). Measurements below 20 keV show that X-ray bursters, representing weakly magnetized neutron stars (NSs), also have power law tails. As in the BHCs, there is a hardness/flux anticorrelation, clearly observed in a number of bursters: e.g. 4U 1636-536 (Breedon et al. 1986), 4U 1735-444 (Smale et al. 1986), 4U 1705-44 (Langmeier et al. 1987), 4U 1608-522 (Mitsuda et al. 1989) and 4U 0614+091 (Barret and Grindlay 1995).

Until recently, most observations of accreting NSs have been limited to less than 20 keV. A notable exception was the detection of a 150 day outburst from the burster Cen X-4 with SIGNE 2 MP/PROGNOZ 7 (Bouchacourt et al. 1984) in the 3–163 keV band. In this observation the hard X-ray flux was high both at the beginning and end of the outburst when the soft X-ray flux was low. With observations by SIGMA, the situation has changed and many more X-ray bursters are now detected above 20 keV (Barret and Vedrenne 1994). The hard X-ray emission is typically variable on the time scale of days and seems to be detected preferentially from the low luminosity bursters. Additional bursters are being detected in hard X-rays with BATSE monitoring (see Barret et al. 1996). Numerous X-ray bursters are now firmly established as

sources of hard X-ray emission.

4U 0614+091 is one of the low luminosity bursters. It was previously identified as an X-ray burster (Swank et al. 1978; Brandt et al. 1992; Brandt 1994) and as a probable atoll source (Singh and Apparao 1995). BATSE monitoring has revealed numerous episodes of transient emission above 20 keV from 4U 0614+091 (Ford et al. 1996a).

Here we describe the simultaneous observations of 4U 0614+091 using the Burst and Transient Source Experiment (BATSE) aboard the Compton Gamma-Ray Observatory (CGRO) and the All Sky Monitor (ASM) onboard the Bruno B. Rossi X-ray Timing Explorer (RXTE). In April 1996, with near real-time BATSE monitoring, we discovered an episode of hard X-ray activity from 4U 0614+091 which was between 4 and 15 days long. This event provided a trigger for RXTE pointings on TJD 10195 and 10197, the results of which will be presented elsewhere (Ford et al. 1996b). The correlated ASM and BATSE observations presented here cover this April 1996 event. In Section 2 we describe the observations by both instruments. In Section 3 we discuss the implications of these new results.

2. Observations

The analysis with BATSE uses the technique of Earth occultation, described for example in Harmon et al. (1992) and Zhang et al. (1993). This method offers a 20–150 keV 3σ sensitivity for two week integrations of approximately 1.7×10^{-2} ph cm⁻² s⁻¹ (50 mCrab). With favorable detector geometries (when a source is near a detector normal) the sensitivity can improve to approximately 1.5×10^{-2} ph cm⁻² s⁻¹ in only 2 days.

The ASM has been fully operational since early February 1996 (\sim TJD 10132), following the launch of RXTE in December 1995. The ASM consists of three Scanning Shadow Cameras (SSCs) which scan the sky about 7 times each day. The ASM detectors are position-sensitive proportional counters placed below coded masks. X-ray intensity measurements are derived from the deconvolution of overlapping mask shadows from each X-ray source in the the field of view. The position histograms for each camera are separately recorded in 3 energy bands (1.3-3.0 keV, 3.0-4.8 keV, and 4.8-12.2 keV). The data are processed through standard filters such as a 75° cut on the Earth angle. In addition, for this analysis we consider only on-source dwells in which 4U 0614+091 is the only source in the field of view. The fine details of the instrument calibration are still being refined, and the present analysis is subject to a systematic error of about 3% for uncrowded source regions as inferred from the rms deviations observed in the Crab Nebula. Further details of the instrument and the data analysis methods are provided by Levine et al. (1996).

The 4U 0614+091 light curves are shown in Figure 1. Integrating the BATSE fluxes (Figure 1a) over TJD 10178–10196, the source is detected at a significance of 5.7σ . To confirm that the BATSE light curve is not contaminated by interfering sources, we have produced maps of the region around 4U 0614+091 during the time of the activity. Maps are generated with the occultation technique by producing rate histories over a grid of points (see Ford et al. 1996a). The maps show an obvious enhancement centered on the position of 4U 0614+091, clearly separated from the Crab which lies approximately 17° away. At periodic intervals, the limbs passing through

4U 0614+091 also sweep over the Crab. This occurs for about 25 days prior to TJD 10174 and after TJD 10197. At these times there is no information on the hard X-ray flux.

Figure 1b shows the ASM light curve (3.0–12.2 keV) binned into 0.8 day averages contemporaneous with the BATSE activity. Two separate outburst peaks are clearly visible at TJD 10175 and 10191. The gap in the ASM coverage near TJD 10185 was caused by scheduling problems in the RXTE operations.

A striking feature of Figure 1 is the anticorrelation of the BATSE flux with the ASM count rate. This anticorrelation is exhibited more clearly in Figure 2, which uses a common time binning of 2.0 days for the hard and soft fluxes. The anticorrelation is robust to changes in the energy bands.

We can define hardness ratios for the ASM fluxes, using the rates in the 1.3–3.0, 3.0–4.8 and 4.8–12.0 keV bands (R_1 , R_2 , and R_3 respectively). The R_3/R_1 hardness ratio is shown in Figure 1c. R_3/R_1 , and also the other hardness ratios, do not show a significant correlation with the source intensity. Color-color diagrams of the ASM data indicate that we can not rule out a small contribution from a 1.0–1.5 keV blackbody as in Barret and Grindlay (1995).

We have produced spectra from the ASM and BATSE data in the window TJD 10178–10190. During this entire interval the source is in a ‘hard’ state; the ASM count rate is low while the BATSE flux reaches a peak. To generate the ASM spectrum, count rates were converted to fluxes by normalizing to the Crab rates as observed by the ASM over the same period. The flux errors are calculated from the observed (gaussian) distribution of the Crab count rate. For a conservative error estimate, we use the 3σ value of the Crab

rate distribution. The resulting flux errors for 4U 0614+091 are approximately 10% in the log-log space used for spectral fitting. A power law fit to the three ASM bins yields a spectral index of 2.23 ± 0.33 ($\chi^2_\nu = 0.5$). The low χ^2 results from the conservative flux error estimate. The averaged ASM spectrum corresponds to a 1–20 keV flux of 1×10^{-9} erg cm $^{-2}$ s $^{-1}$ with an implied luminosity of 1×10^{36} erg s $^{-1}$ at 3 kpc.

The BATSE data in the same time window can be fit by a power law with photon index 2.68 ± 0.35 ($\chi^2_\nu = 1.1$). This fit is consistent with the spectra from an archival BATSE analysis of 4U 0614+091 during hard X-ray emission episodes (Ford et al. 1996a). The BATSE flux is 7×10^{-10} erg cm $^{-2}$ s $^{-1}$ (20–100keV) corresponding to a luminosity of 8×10^{35} erg s $^{-1}$ at 3 kpc.

Figure 3 shows the combined BATSE and ASM spectra in the TJD 10178–10190 window. A single power law with index 2.09 ± 0.08 can describe the combined data ($\chi^2_\nu = 1.1$). The index is harder than either of the two independent fits. We note that this spectral index is consistent with the the range 1.86–2.24 for the low state as observed with EXOSAT (Barret and Grindlay 1995). Although, it is difficult to test more complicated models, we attempt to fit a power law with a cutoff, which is an approximation to the Comptonization model in the optically thin regime. Fitting results are summarized in Table 1.

To test the validity of combining ASM and BATSE spectra we have generated spectra for the Crab over the same time interval. The spectra match to within $\sim 20\%$, the BATSE flux being higher than the ASM flux. The difference has a low ($\sim 1\sigma$) significance. With our conservative error estimates, the ASM fluxes are in agreement with the extrapolated

BATSE fit with a χ^2 of 0.93.

3. Discussion

Taken independently, our results in the soft and hard X-ray bands are consistent with previous observations. From 1–20 keV, 4U 0614+091 has been observed before at similar luminosities; e.g. 5×10^{36} erg s $^{-1}$ at 3 kpc with EXOSAT (Barret and Grindlay 1995). In the hard X-ray band, numerous episodes of emission, similar to this one, have been identified in BATSE monitoring (Ford et al. 1996a). Also similar to what we find here, variability has been recorded by factors of approximately 5 on time scales of days. The 20–100 keV flux extrapolated from the EXOSAT spectrum in a high state falls a factor of 4 below the peak of the present hard X-ray outburst, and would not be detectable by BATSE. The EXOSAT low state is closely matches the BATSE and ASM detections during the hard X-ray episode (Figure 3).

This observation of 4U 0614+091 is unique for its simultaneous broad-band coverage. The most notable feature is the clear soft/hard X-ray anticorrelation (Figure 2), which confirms a qualitative trend of anticorrelation noted earlier at lower energies in 4U 0614+091 and other bursters. The observed soft/hard anticorrelation indicates that either the soft or the hard X-ray emission is not a direct measure of the mass accretion rate. Analyzing short segments of ASM and BASTE data, we have found that the total energy flux in the 1–100 keV band tracks the 1–12 keV flux, while the hard 20–100 keV energy flux remains below 1×10^{-9} ergs cm $^{-2}$ s $^{-1}$ with no observable correlation. This indicates that it is in fact the soft X-ray emission which tracks the mass accretion, as is usually assumed. The hard X-ray flux then is actually anticorrelated with

mass accretion rate, and is most likely a manifestation of a special property of the accretion disk. We note that in black hole candidates, for example Cyg X-1 (Crary et al. 1996), the hard X-ray emission is also believed to be anticorrelated with the mass transfer rates.

Both thermal (Comptonization) and non-thermal models of emission can be considered in explaining the hard X-ray emission properties of 4U 0614+091. A thermal model (e.g. Sunyaev and Titarchuk 1980) could account for the hard/soft anticorrelation in the following way: when the soft X-ray flux increases, the Comptonizing plasma cools, resulting in a decreased temperature and hard X-ray flux. Non-thermal models have also predicted hard X-ray emission from neutron stars (Kluźniak et al. 1988) and may explain our results. In non-thermal models, the soft/hard X-ray anticorrelation is the result of the suppression of particle acceleration by inverse Compton cooling caused by an enhanced soft X-ray background. Only for intermediate/low values of L_s can the hard X-ray emission manifest itself as a consequence of a non-thermal particle energy distribution function of energized particles in the disk (Tavani and Liang 1996).

These 4U 0614+091 results are a complement to recent observations of the X-ray burster 4U 1608-522 (Zhang et al. 1996). 4U 1608-522 showed a bright (~ 100 mCrab) outburst in the BATSE light curve lasting approximately 200 days. During this outburst the source was detected by Ginga in a low state, making it the first NS binary in which a low soft X-ray state was definitively linked to a bright phase in hard X-rays. Our observations of 4U 0614+091 extend these results, showing that the hard and soft fluxes are anticorrelated as the source varies. The spectrum

of 4U 1608-522 exhibits a clear break at approximately 65 keV with spectral indices 1.8 and 3.2 ± 0.2 . For 4U 0614+091 the spectra may roll over at a lower energy, which would have important implications for the hard X-ray emission models. This could point, for example, to lower electron temperatures in thermal models.

The present data indicate that when the RXTE pointed observations were performed, on TJD 10195 and 10197, the source was in a low state with a hard power law spectrum ($\alpha \sim 2.1$) and little contribution from a soft component. During these observations we have discovered two high frequency QPOs over the range 580 to 950 Hz (Ford et al. 1996c). The QPO frequency and total count rate are linearly correlated, while the frequency difference between the two peaks is constant. Perhaps the presence of kHz QPOs is linked to the hard X-ray brightness. The two other atoll sources with kHz QPOs, 4U 1728-34 and 4U 1608-52 (Strohmayer et al. 1996, van Paradijs et al. 1996), have also been detected as bright hard X-ray sources by BATSE (Barret et al. 1996).

4. Conclusion

Combining the capabilities of BATSE earth occultation monitoring and the ASM on RXTE, we have measured the flux of 4U 0614+091 over a wide energy band (1–100 keV) during several months. We detected an active hard X-ray phase accompanied by soft X-ray variability. The hard X-ray and soft X-ray fluxes show a distinct anticorrelation. This measurement is an example of the new opportunities now available for broad-band X-ray monitoring.

We would like to acknowledge the BATSE

instrument team and the members of the RXTE Guest Observer Facility for their support and assistance. This work is supported in part by NASA Grants NAG 5-2235 and NGT 8-52806.

REFERENCES

- Barret, D. et al., in 3rd Compton Symposium, Munich, in press (1996)
- Barret, D. and Grindlay, J. ApJ, 440, 841 (1995)
- Barret, D. and Vedrenne, G. ApJS, 92, 505 (1994)
- Bouchacourt, P. et al. ApJ, 285, L67 (1984)
- Brandt, S. PhD Thesis, DSRI (1994)
- Brandt, S. et al. AA, 262, L15 (1992)
- Breedon, L.M. et al. MNRAS, 218, 487 (1986)
- Crary, D.J. et al. ApJ, 462, L71 (1996)
- Ford, E. et al., in preparation (1996a)
- Ford, E. et al., in preparation (1996b)
- Ford, E. et al., IAU Circ. No. 6426 (1996c)
- Harmon, B.A., et al. Compton Observatory Science Workshop, NASA CP 3137, 69 (1992)
- Inoue, H., Adv. in Space Sci., 10(2), 153 (1990)
- Kluźniak, Ruderman, M., Shaham, J., Tavani, M., Nature, 336, 558 (1988)
- Langmeier, A. et al. ApJ, 323, 288 (1987)
- Levine, A.M, Bradt, H., Cui, W., Jernigan, J.G., Morgen, E.H., Remillard, R.A., Shirey, R., Smith, D. ApJL, submitted (1996)
- Levine, A.M. et al. ApJ, 54, 581 (1984)
- Mitsuda, K. et al. PASJ, 41, 111 (1989)
- Singh, K.P. and Apparao, K.M.V. ApJ, 431, 826 (1995)
- Smale, A.P., Corbet, R.H.D., Charles, P.A., Menzies, J.W., and Mack, P. MNRAS, 223, 207 (1986)
- Strohmayer, T. et al., IAU Circ. No. 6320 (1996)
- Sunyaev, R.A. and Titarchuk, L. AA, 86, 121 (1980)
- Swank, J.H. et al. MNRAS, 182, 349 (1978)
- Tanaka, Y., in Proc. of the 23rd ESLAB Symposium, Vol. 1, ed. J.Hunt (ESA Pub. Div.), 3 (1989)
- Tavani, M. and Liang, E., in 3rd Compton Symposium, Munich, in press (1996)
- van der Klis, M. ApJS, 92, 511 (1994)
- van Paradijs, J. et al., IAU Circ. No. 6336 (1996)
- Zhang, S.N., et al., Nature, 366, 245 (1993)
- Zhang, S.N. et al., in 3rd Compton Symposium, Munich, in press (1996)

This 2-column preprint was prepared with the AAS L^AT_EX macros v4.0.

TABLE 1
SPECTRAL FITS

Model: Data	α	A_0 [$\times 10^{-3}$]	χ^2, ν
PL: BATSE	2.68 (0.35)	7.05 (3.57)	1.1, 3
PL: ASM	2.23 (0.33)	2.30 (1.06)	0.5, 1
PL: BATSE+ASM	2.09 (0.08)	2.92 (0.32)	1.1, 6
CUTOFFPL: BATSE+ASM	1.79 (0.18)	3.83 (0.97)	1.8, 5
	$E_c = 45(20)$ keV		

NOTE.—Fits to data in the interval TJD 10178–10190. The spectral fits are of the form, PL: $A_0(E/10 \text{ keV})^{-\alpha}$, CUTOFFPL: $A_0(E/10 \text{ keV})^{-\alpha}e^{-E/E_c}$ ($\text{ph cm}^{-2} \text{ s}^{-1} \text{ keV}^{-1}$). Errors (parenthesis) are 1σ .

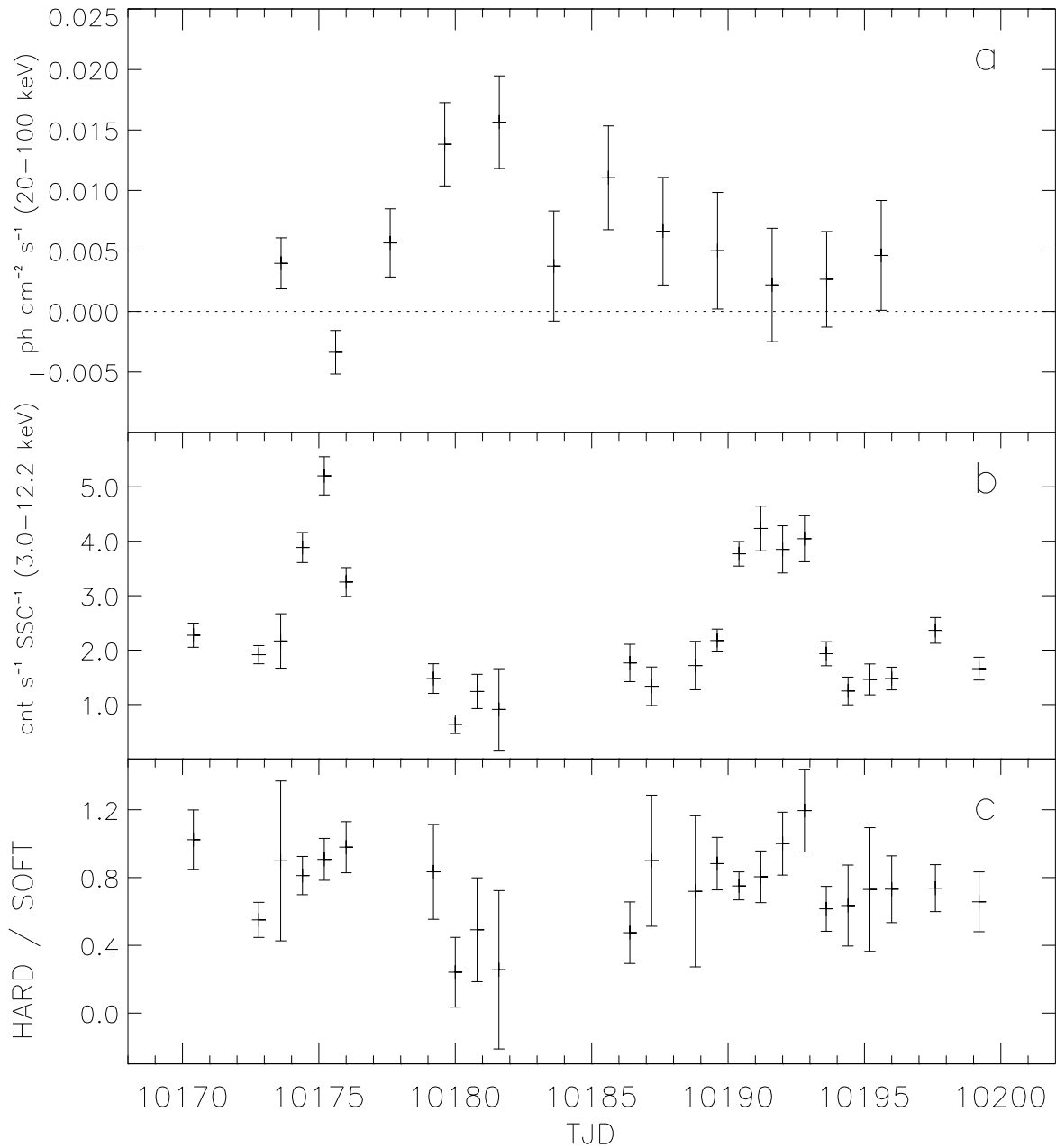


Fig. 1.— Combined BATSE (a) and ASM/RXTE (b) light curves. The BATSE and ASM data are binned in 2 and 0.8 day bins respectively. The BATSE rate to flux conversion assumes a power law spectrum with index 2.8. The $[4.8\text{--}12.0 \text{ keV}]/[1.3\text{--}3.0 \text{ keV}]$ hardness ratio from the ASM data is shown in (c). Truncated Julian Day (TJD) 10175 corresponds to 2 April 1996.

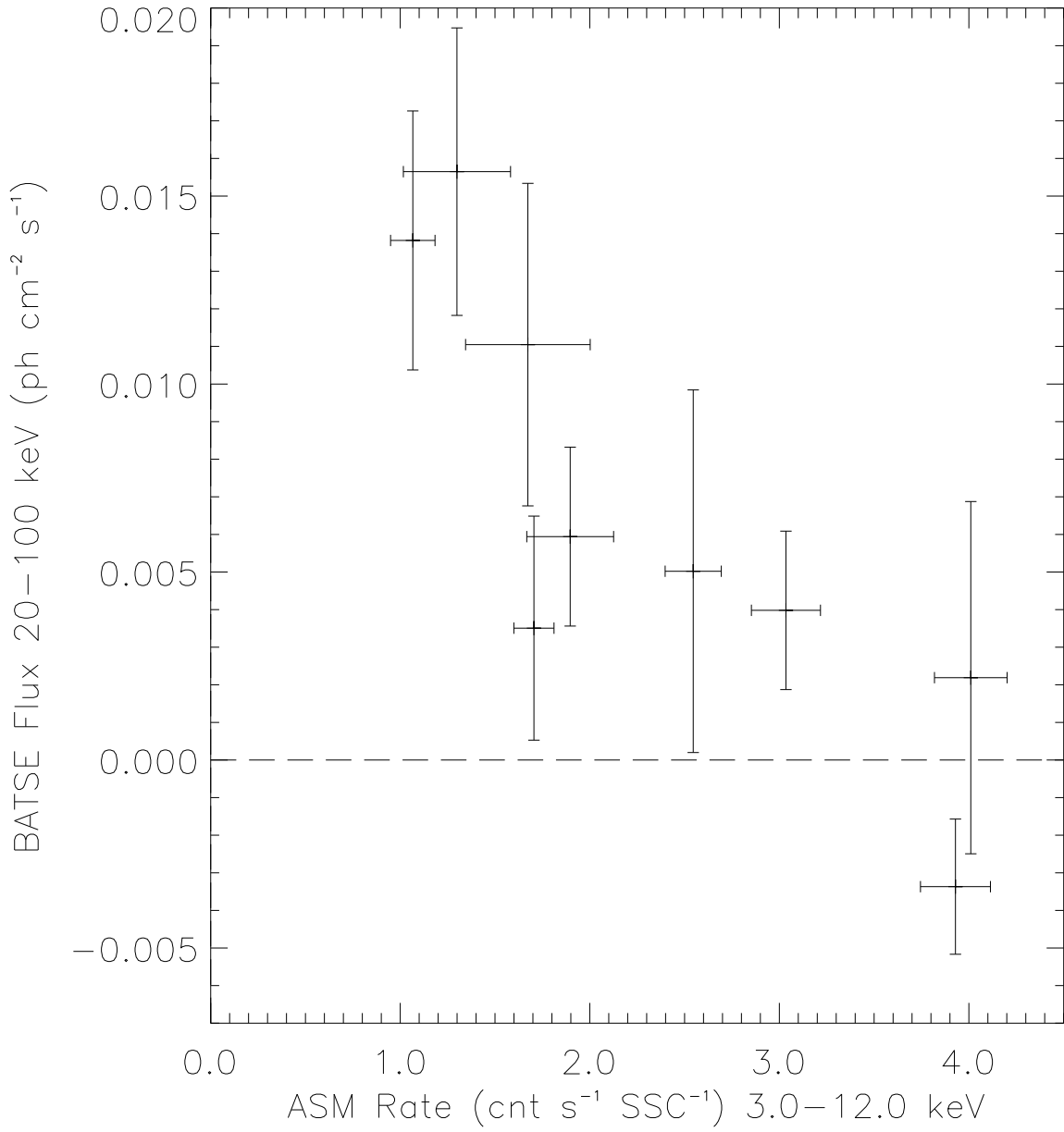


Fig. 2.— BATSE 20–100 keV flux vs ASM 3.0–12.0 keV count rate. Data are binned in matching 2 day intervals.

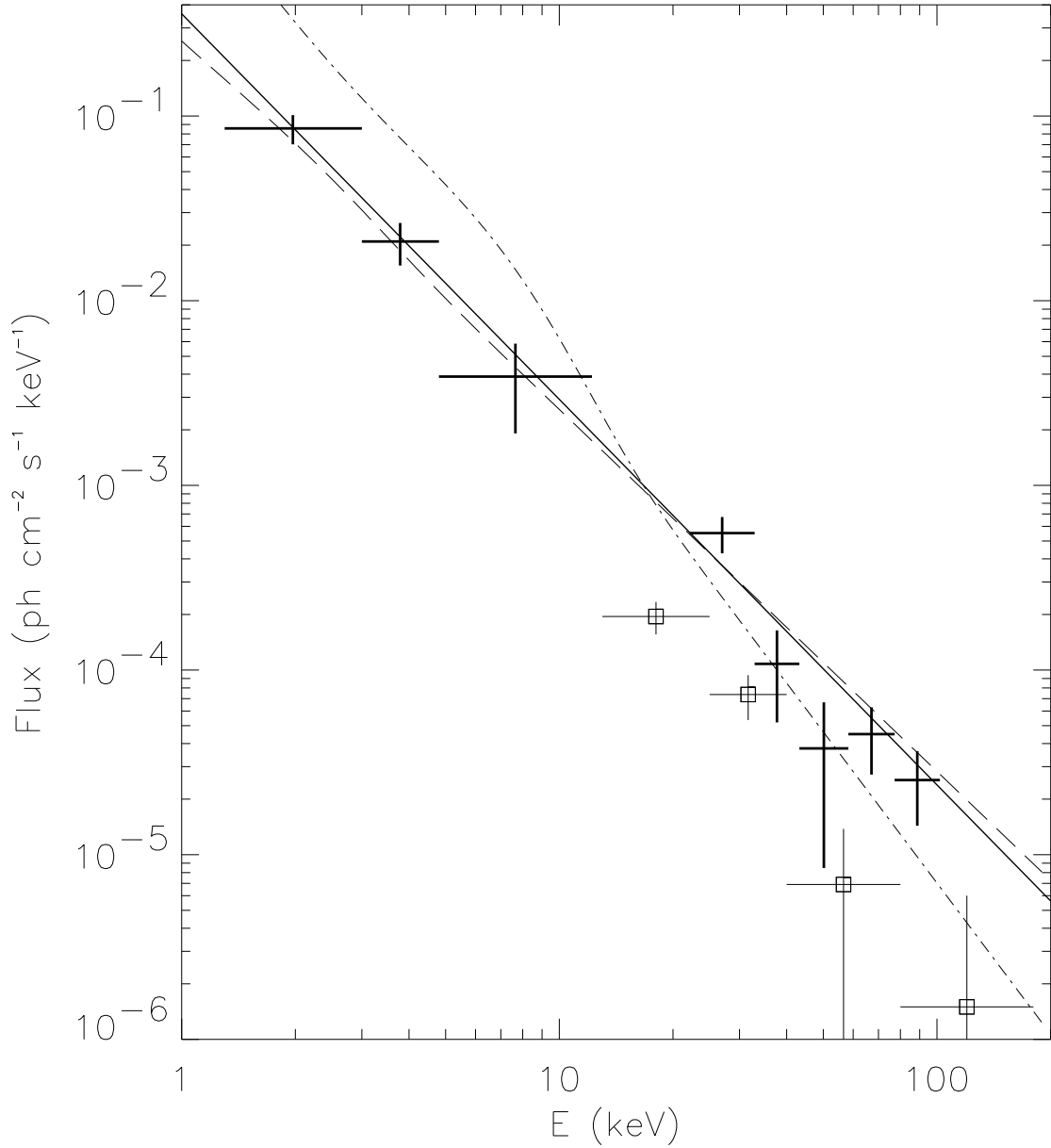


Fig. 3.— Combined BATSE and ASM spectrum over the period TJD 10178–10190. The solid line is the single power law fit ($\alpha = 2.09 \pm 0.08$) to the ASM and BATSE fluxes. The dashed (dot-dash) lines show the low (high) states as identified by EXOSAT. These are extrapolated above the EXOSAT limit of 15 keV. Squares are measurements by HEAO-1 A4 from Levine et al. (1984).